


# The autonomic nerves around the vein of Marshall: a postmortem study with clinical implications

DENIS DEPES,<sup>1,2,\*</sup>  ARI MENNANDER,<sup>2,3</sup> PAAVO IMMONEN,<sup>1,2</sup> ARTTURI MÄKINEN,<sup>1</sup>  
HEINI HUHTALA,<sup>4</sup> TIMO PAAVONEN<sup>1,2</sup> and IVANA KHOLOVÁ<sup>1,2</sup>

<sup>1</sup>Department of Pathology, Fimlab Laboratories; <sup>2</sup>Faculty of Medicine and Health Technology, Tampere University; <sup>3</sup>Division of Cardiothoracic Surgery, Tampere University Heart Hospital; and <sup>4</sup>Faculty of Social Sciences, Tampere University, Tampere, Finland

Depes D, Mennander A, Immonen P, Mäkinen A, Huhtala H, Paavonen T, Kholová I. The autonomic nerves around the vein of Marshall: a postmortem study with clinical implications. APMIS. 2024.

This study aims to analyze the vein of Marshall (VOM) in human autopsy hearts and its correlation with clinical data to elucidate the morphological substrates of atrial fibrillation (AF) and other cardiac diseases. Twenty-three adult autopsy hearts were studied, assessing autonomic nerves by immunohistochemistry with tyrosine hydroxylase (sympathetic nerves), choline acetyltransferase (parasympathetic nerves), growth-associated protein 43 (neural growth), and S100 (general neural marker) antibodies. Interstitial fibrosis was assessed by Masson trichrome staining. Measurements were conducted via morphometric software. The results were correlated with clinical data. Sympathetic innervation was abundant in all VOM-adjacent regions. Subjects with a history of AF, cardiovascular cause of death, and histologically verified myocardial infarction had increased sympathetic innervation and neural growth around the VOM at the mitral isthmus. Interstitial fibrosis increased with age and heart weight was associated with AF and cardiovascular cause of death. This study increases our understanding of the cardiac autonomic innervation in the VOM area in various diseases, offering implications for the development of new therapeutic approaches targeting the autonomic nervous system.

**Key words:** Cardiac autonomic nervous system; interstitial fibrosis; cardiovascular cause of death; atrial fibrillation; vein of Marshall.

Denis Depes, Faculty of Medicine and Health Technology, Tampere University, Arvo Ylpön katu 34, 33520 Tampere, Finland. e-mail: [denis.depes@tuni.fi](mailto:denis.depes@tuni.fi)

The ligament of Marshall (LOM) is an embryological remnant of a left superior caval vein located obliquely above the left atrial appendage in the left lateral ridge laterally to the left superior pulmonary vein [1]. The LOM contains the vein of Marshall (VOM) [1], myocardial fibers, and vascular, and nerve structures [2]. The LOM is a potential source of atrial fibrillation (AF), forming a portion of non-pulmonary vein AF triggers [1]. The VOM, as a patent remnant draining the posterior and posterolateral wall of the left atrium into the coronary sinus, provides a suitable endovascular route for ablation techniques that can effectively eliminate AF triggers [3].

Atrial interstitial fibrosis plays an important role in myocardial remodeling and contributes to increased cardiovascular morbidity and mortality [4],

however, the mechanisms are still not fully understood. Previous studies have suggested that atrial interstitial fibrosis may be associated with vulnerability to arrhythmias [5], heart failure, and aging [6].

In the human heart, the LOM area was shown to contain sympathetic and parasympathetic nerves and ganglia [2]. Although some morphometric studies have been performed on LOM/VOM, no histological studies have explored the complexity of autonomic innervation and fibrosis in relation to AF and cardiovascular causes of death.

This study provides a detailed morphometric analysis of autonomic nerve density and interstitial fibrosis around the VOM at the level of the mitral isthmus in autopsied human hearts. The morphological changes were correlated to clinical data, and the findings may contribute to the understanding of the relations between VOM autonomic innervation

Received 30 March 2023. Accepted 31 January 2024

and fibrosis, and cardiac diseases. Although VOM studies are therapeutically relevant as the VOM is a suitable target for endovascular ablation techniques [3, 7, 8], the mechanisms of AF remain elusive and necessitate further research to fill the knowledge gap [9].

## METHODS

### Series characterization and specimens collection

Twenty-three human hearts were collected from hospital autopsies. The mean age  $\pm$  standard deviation (SD) of the subjects (11 females, 12 males) was  $74 \pm 12$  years (range 39–95). The mean heart weight  $\pm$  SD was  $447 \pm 117$  grams. According to the autopsy referrals, heart rhythm data were available in 18 subjects (78.3%): 7 subjects had a history of AF, and 11 had no history of AF. Eight subjects had documented underlying cardiovascular causes of death, and 7 subjects had documented immediate cardiovascular causes of death. Coronary atherosclerosis was classified according to the AECVP guidelines [10, 11]. Briefly, gross examination of the patency of coronary arteries was made by the eye as no stenosis (<30%), mild (30%–50%), moderate (50%–75%), and severe (>75%)

grade luminal stenosis. Gross assessments of focal lesions were confirmed by histology. Detailed clinical and autopsy data are given in Table 1.

The VOM with adjacent tissue was dissected from autopsy hearts. The coronary sinus ostium was approached from the right atrium, and a longitudinal section along the coronary sinus was performed. The VOM ostium was identified at the level of the Vieussens valve, and its course and length were determined with a metal probe (diameter 1 mm). A tissue sample consisting of the VOM and surrounding tissue was excised, reaching from the VOM ostium until the vein patency allowed insertion of the probe as distally as possible to the VOM. The samples were fixed in 10% formalin, cut into 5 mm thick slices, and processed into individual paraffin blocks. In total, 146 blocks of VOM tissue were included in the study, ranging from 5 to 9 blocks per subject based on the heart size (Fig. 1).

### Special stains and immunohistochemistry

Serial 5- $\mu$ m-thick sections were cut from all paraffin blocks. Hematoxylin–eosin stained sections were used to identify the VOM in each block. Altogether, 146 sections from paraffin blocks with identified VOM were stained with Masson's trichrome (Sigma, Merck Life Science,

**Table 1.** Series characteristics

ID no.	Age	Heart weight (g)	Sex	Heart rhythm	Underlying cause of death	Immediate cause of death	Coronary atherosclerosis	MI
1	71	450	F	AF-	Liver cirrhosis	Esophagus varix bleeding	Moderate	–
2	85	344	M	AF-	Heart hypertrophy	Pulmonary edema	Mild	–
3	85	580	M	AF-	Schwannoma of cerebellum-pons area	Ischemia of cerebral hemisphere and cerebellum	Moderate	–
4	73	372	F	AF-	Alzheimer's disease	Pneumonia	Severe	–
5	71	365	F	AF+	Hemorrhagic gastroenteritis	Hemorrhagic gastroenteritis	Mild	–
6	39	357	M	AF-	Pulmonary embolism	Pneumonia	Not present	–
7	76	405	M	NA	Alzheimer's disease	Bronchopneumonia	Severe	–
8	69	446	M	AF-	Acute necrotic pancreatitis (cholecystolithiasis etiology)	Necrotic hemorrhagic peritonitis	Mild	–
9	82	450	F	AF+	Coronary artery disease	Coronary artery disease	Severe	–
10	90	589	F	AF+	Coronary artery disease	Pneumonia	Severe	–
11	95	473	M	AF+	Heart amyloidosis	Cardiac failure	Severe	–
12	84	545	M	AF-	Chronic lymphatic leukemia	Myocardial infarction	Moderate	+
13	65	677	M	AF+	Dilated cardiomyopathy	Cardiac failure	Mild	–
14	51	407	M	AF-	Liver cirrhosis	Pneumonia	Mild	+
15	73	414	F	AF-	Ileocecal strangulation	Sepsis	Mild	+
16	63	500	F	NA	Brain stem hemorrhage	Brain stem hemorrhage	Moderate	–
17	79	552	M	NA	Coronary artery disease	Myocardial infarction	Severe	+
18	63	280	F	AF-	Granulomatosis with polyangiitis	Pneumonia	Not present	–
19	72	520	M	AF+	Chronic obstructive pulmonary disease	Cardiac failure	Not present	+
20	75	663	M	AF+	Coronary artery disease	Myocardial infarction	Severe	+
21	77	256	F	NA	Liver necrosis	Pneumonia	Not present	+
22	70	335	F	AF-	Small intestine T-cell lymphoma	Small intestine T-cell lymphoma	Moderate	–
23	83	301	F	NA	Combination of Alzheimer's and dementia with Lewy's bodies	Pneumonia	Not present	+

AF<sup>-</sup>, no history of atrial fibrillation; AF<sup>+</sup>, history of atrial fibrillation; F, female; M, male; MI, myocardial infarction; NA, not available.

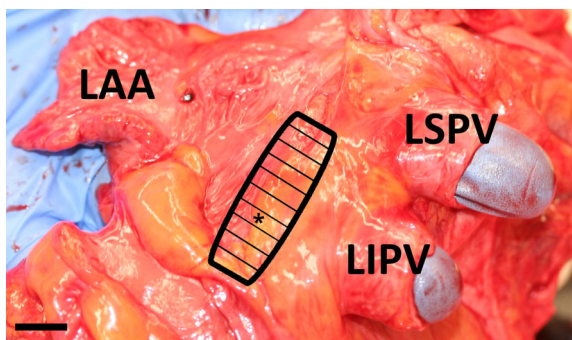


**Fig. 1.** Macroscopic photograph of the fresh autopsy heart. The LOM/VOM dissection and sampling region are marked with bars. The area selected for further immunohistochemical studies is determined with an asterisk and corresponds to the epicardial view of the mitral isthmus area. LAA, left atrial appendage; LIPV, left inferior pulmonary vein; LSPV, left superior pulmonary vein. Scale bar = 1 cm.

Espoo, Finland) to evaluate interstitial fibrosis. One paraffin block of each subject, determined by the position of the left inferior pulmonary vein containing the mitral isthmus with microscopically identified VOM, was selected for further immunohistochemical analysis. The main distance  $\pm$  SD from the VOM ostium to the selected region was  $21.52 \pm 7.3$  mm.

The following primary antibodies were used: S100 (dilution 1:6000, Z0311, Dako Denmark A/S, Glostrup, Denmark) as a general neural marker, growth-associated protein 43 (GAP43; dilution 1:100, AB5220, Chemicon, Merck KGaA, Darmstadt, Germany) as a neural growth marker, tyrosine hydroxylase (TH; dilution 1:100, AB152, Chemicon, Merck KGaA) as a marker of sympathetic nerves and ganglia, and choline acetyltransferase (CHAT; dilution 1:300, AB143, Chemicon, Merck KGaA) as a

marker of parasympathetic nerves and ganglia. The immunohistochemical staining was done using the Ventana Automatic System (Ventana Medical Systems, Tucson, AZ, USA), as previously described [12, 13].

### Morphometric analysis

The stained sections were scanned by a NanoZoomer-XR scanner (Hamamatsu Photonics, Hamamatsu, Japan) at  $40\times$  magnification, and the morphometric measurements were done using open-source software for bioimage analysis (QuPath, Queens University, Belfast, Northern Ireland [14]). The areas ( $\text{mm}^2$ ) of the whole slide, myocardium area, and non-myocardial fibrotic and fatty tissue area were measured. In addition, four regions adjacent to the identified VOM were defined within the expansion radius of 250, 500, 1000, and 1500  $\mu\text{m}$  (Fig. 2A–D).

### Nerve quantity and density

Positive nerves and ganglia were manually selected with eye control of the nerve histological pattern at  $20\times$  magnification. The distribution of autonomic nerves was evaluated in seven separate regions within each slide (whole slide, myocardium, fibro-fatty tissue, four expansion radius regions adjacent to the VOM). The nerve density was quantified by manual counting of positive nerves and ganglia per region (nerves/ $\text{mm}^2$  – data included in results) and by measuring the positively stained nerve tissue area per region ( $\mu\text{m}^2/\text{mm}^2$  – data included in the supplementary material). All measurements were performed individually in S100-, GAP43-, TH-, and CHAT-stained sections (Fig. 3A).

### Interstitial fibrosis quantification

Interstitial myocardial fibrosis was quantified by semiautomated image analysis. The pixel classifier, an artificial intelligence-guided function, was used to detect fibrosis and cardiomyocytes by setting thresholds specific for blue-

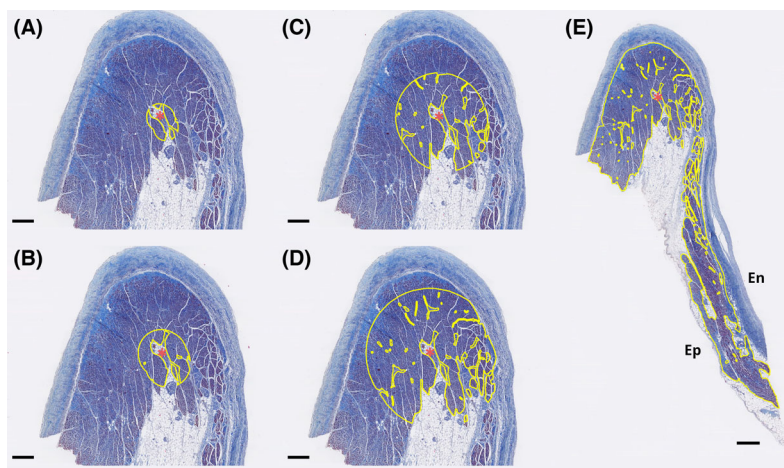


**Fig. 2.** Regions of interest. A transverse section of the vein of Marshall (VOM) (red asterisk) including adjacent myocardial areas (yellow) after manual exclusion of perivascular areas, vessels, nerves, and staining artifacts. (A) Expansion radius of 250  $\mu\text{m}$  from VOM. (B) Expansion radius of 500  $\mu\text{m}$  from VOM. (C) Expansion radius of 1000  $\mu\text{m}$  from VOM. (D) Expansion radius of 1500  $\mu\text{m}$  from VOM. (E) The myocardium of the whole slide containing VOM. En, endocardial surface; Ep, epicardial surface. Stain: Masson's trichrome. Scale bars: A–D = 500  $\mu\text{m}$ , E = 800  $\mu\text{m}$ .

(collagen) and red-stained (myocytes) components in Masson trichrome-stained sections. The classifier had been trained on multiple images before being used for the analysis. The settings were adjusted according to the tutorials provided by the software developer [14]. The area (in  $\mu\text{m}^2$ ) and percentage of the fibrotic tissue were evaluated. To assess only interstitial fibrosis, manual exclusion of perivascular areas, vessels, nerves, and staining artifacts was performed at 15 $\times$  magnification in each section. Measurements were done in five regions within each slide (whole myocardium and four expansion radius regions adjacent to the VOM, including only myocardial tissue as shown in Fig. 2).

### Statistical analysis

Continuous variables were expressed as mean  $\pm$  SD or as median  $\pm$  interquartile range value (IQR) and compared using a Student *t*-test, Mann–Whitney *U*-test, or ANOVA test followed by *post hoc* multiple comparison tests with Bonferroni correction, as appropriate. Categorical variables were expressed as the count and percentage. Spearman's correlation coefficient (*r*) was used for analyzing the correlation between interstitial fibrosis and age. The normality of data distribution was evaluated using the Shapiro–Wilk test. Statistical Package for the Social Sciences version 24.0 (SPSS Inc., Chicago, IL, USA) was used to perform

the statistical analysis and a two-tailed *p*-value of  $<0.05$  was considered significant.

### Ethical statement

The study was approved by the Pirkanmaa Health Care District Ethical Committee (R15013), and the use of tissue samples was approved by Valvira. The consent of the individuals was waived. The study protocol is in accordance with the Declaration of Helsinki.

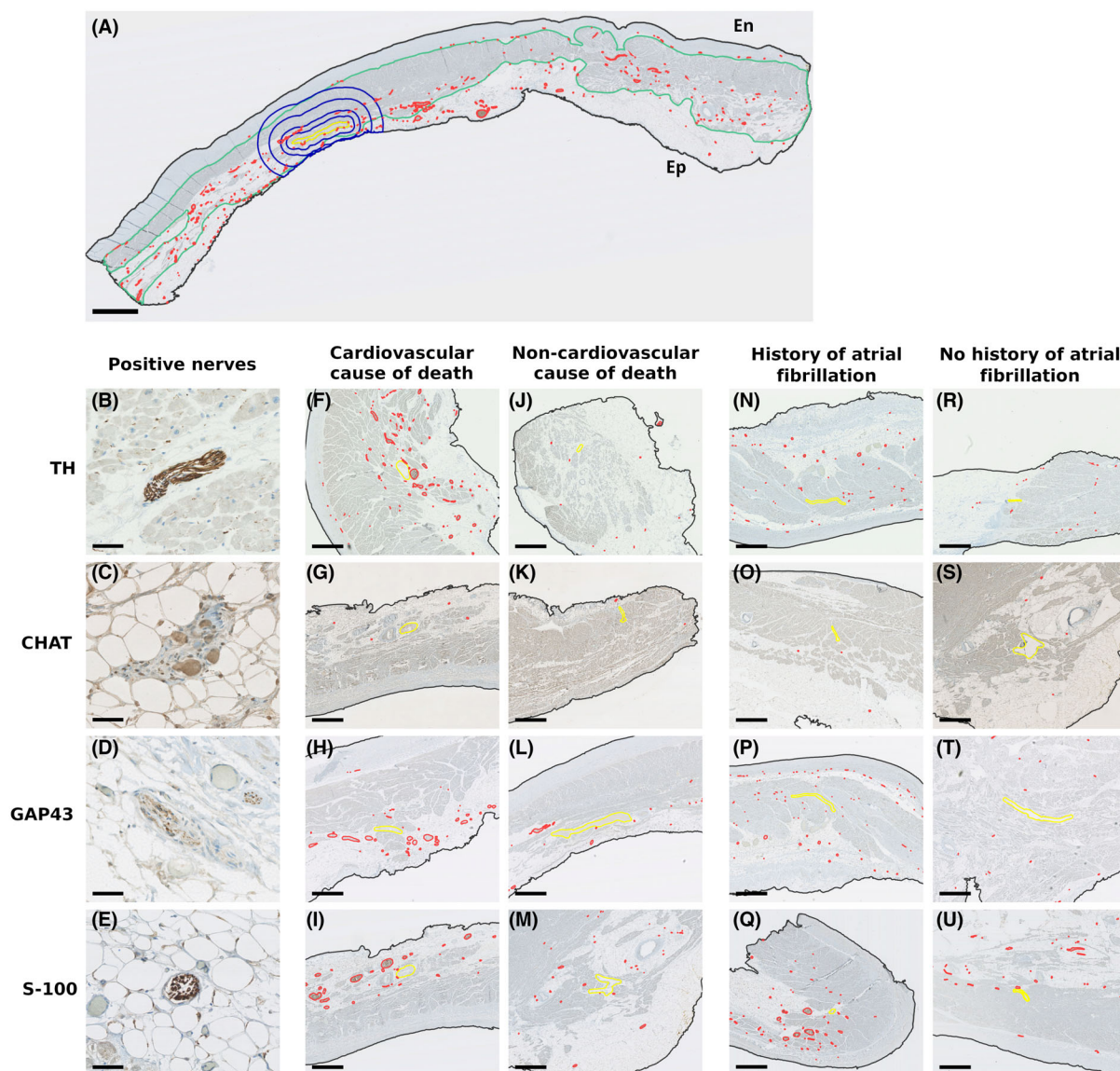
## RESULTS

### Subjects' characteristics

In total, 23 adult autopsy hearts were studied. Heart rhythm data were available in 18 subjects. The mean heart weight ( $\pm$ SD) was significantly higher in subjects with a history of AF ( $n = 7$ ) than in those with no history of AF ( $n = 11$ ) ( $533.86 \pm 115.22$  g vs  $411.82 \pm 90.08$  g;  $p = 0.023$ ). Males had a significantly higher mean heart weight compared to females ( $497.42 \pm 110.97$  g vs  $392 \pm 100.69$  g;  $p = 0.027$ ). Subjects with documented immediate cardiovascular causes of death had increased heart weight compared to those with non-

**Fig. 3.** Overview, general findings, and comparison of immunohistochemical sections containing the vein of Marshall (VOM) in subjects with documented cardiovascular vs non-cardiovascular cause of death and atrial fibrillation vs without atrial fibrillation. (A) Low-power representative figure demonstrating an oblique section of the VOM (labeled in yellow) with all seven studied regions and innervation. Positive nerves and ganglia are labeled in red and they can be found in all the studied regions of interest—the whole slide (labeled in black), myocardium (labeled in green), and four myocardial regions (labeled in blue) within 250, 500, 1000, and 1500  $\mu\text{m}$  expansion radiuses adjacent to the VOM. (B–E) High-power representative sections of positive autonomic nerves and ganglia. (B) A tangential section of TH-positive nerve in sparse fatty tissue is surrounded by myocardial bundles. (C) A transverse section parasympathetic ganglion is surrounded by adipose tissue. (D) An oblique section of two GAP43-positive nerves found in the fibro-fatty tissue. (E) A transverse section of an S100-positive nerve is fully surrounded by fatty cells. (F–U) Sections with a focus on the area around the VOM (labeled in yellow) and adjacent nerves (red). (F) A transverse section of the VOM is surrounded by abundant TH-positive nerves throughout the myocardium and fibro-fatty tissue. (G) Left atrial myocardium with surrounding fibro-fatty tissue on the epicardial side with only a few CHAT-positive nerves in the transversely sectioned VOM area. (H) A rich GAP43-positive nerve density is in the fibro-fatty tissue surrounding the obliquely sectioned VOM, in the myocardium fewer nerves can be observed. (I) A transverse section of the VOM adjacent to the fibro-fatty tissue containing numerous S100-positive nerves. (J) An abundant fatty replacement of the myocardium containing the transversely sectioned VOM and only sporadic TH-positive nerves. (K) A transverse section of the VOM located in the myocardial tissue with only two adjacent CHAT-positive nerves. (L) A longitudinal section of the VOM surrounded by sparse GAP43-positive nerves, which are partially located in the fibro-fatty tissue area. (M) A transverse section of the VOM located within a myocardial bundle. A vessel is located in the adjacent fatty-fibro tissue. S100-positive nerves are present in all compartments. (N) TH-positive nerves detected throughout the myocardium and fibro-fatty tissue around the longitudinally sectioned VOM. (O) An oblique section of the VOM embedded in the myocardium with only a few detected CHAT-positive nerves. (P) Dense GAP43-positive innervation is in both the myocardium and fibro-fatty tissue around the longitudinally sectioned VOM. (Q) Numerous S100-positive nerves are in both the myocardium and fibro-fatty tissue surrounding the transversely sectioned VOM. (R) Myocardium and adipose tissue surrounding the obliquely sectioned VOM with sparse TH-positive nerves. (S) A transverse section of the VOM within a myocardial bundle is surrounded by the fibro-fatty tissue and a larger vessel in the right upper part of the figure. Only a few CHAT-positive nerves can be detected. (T) Sparse GAP43-positive nerves in the myocardium with a fatty replacement in the longitudinally sectioned VOM area. (U) A transverse section of the VOM and numerous S100-positive nerves within the myocardium with fatty replacement. En, endocardial surface; Ep, epicardial surface. Stains: A, E, I, M, Q, U—S100 immunohistochemistry (a general neural marker); B, F, J, N, R—tyrosine hydroxylase immunohistochemistry (a marker of sympathetic nerves); C, G, K, O, S—choline acetyltransferase immunohistochemistry (a marker of parasympathetic nerves); D, H, L, P, T—growth-associated protein 43 immunohistochemistry (a neural growth marker). Scale bars: A = 2 mm, B–E = 50  $\mu\text{m}$ , F–U = 1 mm.





cardiovascular causes of death ( $554.29 \pm 87.2$  g vs  $400.06 \pm 96.32$  g;  $p = 0.002$ ). No other differences were found among subjects and available clinical data (age, sex, heart weight, heart rhythm, cause of death, presence of coronary atherosclerosis, dilatation of heart compartments, and myocardial infarction).

#### Pathological heart findings

Left ventricular hypertrophy was found in 22 subjects, and heart compartments dilatation was present in nine subjects. Severe coronary atherosclerosis was present in seven hearts, moderate in 5, mild in 6, and coronary

atherosclerosis was not present in five studied hearts. Myocardial infarction was histologically diagnosed in 8 subjects (Table 1). Moreover, dilated cardiomyopathy, cardiac amyloidosis, rheumatic heart disease, and chronic lymphatic leukemia infiltration were present in separate cases. Myocardial fat infiltration and disarray were microscopically present in one case.

#### Morphometric analysis

The mean length of the patent VOM  $\pm$  SD from the VOM ostium was  $32.83 \pm 5.18$  mm. Microscopically, the VOM was surrounded by myocardial fibers and fibro-fatty tissue containing vessels.

Nerves and ganglia detected in sections with TH, CHAT, GAP43, and S100 antibodies were located both in the myocardium and fibro-fatty tissue around the VOM (Fig. 3A–E). Co-location of nerves and vascular structures forming neurovascular bundles was commonly found in the studied areas. In the evaluation of interstitial fibrosis, collagen stained in blue by Masson's trichrome stain was detected diffusely in the myocardium. Based on our observation, there were no conduction fibers in the VOM areas.

#### Nerve densities

Detailed data relating to TH-, CHAT-, GAP43-, and S100-positive nerve densities from all seven studied regions around the VOM are shown in

Tables S1–S5. In brief, findings show sympathetic (TH-positive) nerve predominance in the VOM area (Table S1A). Table 2 summarizes only statistically significant results of measured nerve densities. All nerve density values are expressed as median (IQR – interquartile range). The overall whole slide TH-positive nerve density was 1.88 (0.8–2.4) nerves (n)/mm<sup>2</sup> and 3064.71 (1431.17–5063.69) μm<sup>2</sup>/mm<sup>2</sup>, CHAT-positive nerve density was 0.04 (0.01–0.12) n/mm<sup>2</sup> and 81.76 (36.53–229.74) μm<sup>2</sup>/mm<sup>2</sup>, GAP43-positive nerve density was 0.62 (0.42–1.25) n/mm<sup>2</sup> and 2839.01 (575.38–5719.19) μm<sup>2</sup>/mm<sup>2</sup>, and S100-positive nerve density was 1.39 (1.01–1.97) n/mm<sup>2</sup> and 3069.80 (965.78–5731.76) μm<sup>2</sup>/mm<sup>2</sup> in the VOM area.

**Table 2.** Statistically significant results of nerve densities' differences in regions around the vein of Marshall

A: Heart rhythm			Atrial fibrillation		No history of AF		p Value
Marker	Region	Unit	Median	IQR	Median	IQR	
TH	250 μm radius	n/mm <sup>2</sup>	3.63	2.22–11.62	0.68	0–1.95	0.016
	500 μm radius	n/mm <sup>2</sup>	4.58	2.48–7.04	0.85	0.74–1.73	0.013
GAP43	250 μm radius	n/mm <sup>2</sup>	3.51	0–5.32	0.00	0–0.96	0.042
S100	500 μm radius	n/mm <sup>2</sup>	3.41	3.15–7.57	1.30	0.68–4.59	0.026
B: Myocardial infarction			Myocardial infarction		Control		p Value
Marker	Region	Unit	Median	IQR	Median	IQR	
TH	500 μm radius	μm <sup>2</sup> /mm <sup>2</sup>	6975.93	1759.85–32667.28	808.33	172.06–6139.84	0.033
	1500 μm radius	μm <sup>2</sup> /mm <sup>2</sup>	4327.61	1961.08–19001.55	1187.96	252.08–3596.31	0.039
GAP43	250 μm radius	n/mm <sup>2</sup>	3.55	1.03–6.67	0.00	0–1.45	0.006
		μm <sup>2</sup> /mm <sup>2</sup>	2278.55	1285.38–26036.26	0.00	0–503.3	0.006
S100	Myocardium	n/mm <sup>2</sup>	4301.24	2450.32–16032.54	681.96	153.15–2063.37	0.033
		μm <sup>2</sup> /mm <sup>2</sup>	1.20	0.64–2.02	0.45	0.23–1.23	0.039
S100	250 μm radius	n/mm <sup>2</sup>	4686.09	2283.16–8322.07	1047.93	202.19–2857.54	0.045
		μm <sup>2</sup> /mm <sup>2</sup>	5.32	4.46–8.24	1.85	0–3.76	0.011
		n/mm <sup>2</sup>	9872.81	4665.68–35866.06	1576.30	0–8275.98	0.044
S100	500 μm radius	n/mm <sup>2</sup>	5.14	3.7–6.28	1.50	0–3.37	0.028
		n/mm <sup>2</sup>	3.32	2.44–4.41	1.34	0.69–2.8	0.039
S100	1000 μm radius	n/mm <sup>2</sup>	3.32	2.44–4.41	1.34	0.69–2.8	0.039
		μm <sup>2</sup> /mm <sup>2</sup>	3.32	2.44–4.41	1.34	0.69–2.8	0.039
C: Underlying cause of death			Cardiovascular		Non-cardiovascular		p Value
Marker	Region	Unit	Median	IQR	Median	IQR	
TH	500 μm radius	n/mm <sup>2</sup>	3.77	2.42–6.43	0.85	0.56–4.58	0.045
	1000 μm radius	n/mm <sup>2</sup>	2.87	1.38–5.58	1.22	0.75–2.89	0.045
CHAT	Myocardium	n/mm <sup>2</sup>	0.07	0.03–0.13	0.01	0–0.05	0.034
S100	500 μm radius	μm <sup>2</sup> /mm <sup>2</sup>	11516.59	2531.47–61155.31	1653.43	0–5528.76	0.038
D: Immediate cause of death			Cardiovascular		Non-cardiovascular		p Value
Marker	Region	Unit	Median	IQR	Median	IQR	
TH	250 μm radius	n/mm <sup>2</sup>	7.17	2.22–11.62	0.34	0–2.03	0.019
		μm <sup>2</sup> /mm <sup>2</sup>	8730.25	874.29–79034.56	78.86	0–2748.13	0.027
GAP43	500 μm radius	n/mm <sup>2</sup>	4.64	2.9–7.47	0.83	0.58–2.23	0.004
		μm <sup>2</sup> /mm <sup>2</sup>	10053.16	1404.12–70724.08	1125.59	212.38–5626.35	0.032
GAP43	Myocardium	n/mm <sup>2</sup>	5968.53	2795.57–11708.6	2059.63	731.96–3128.29	0.038
		μm <sup>2</sup> /mm <sup>2</sup>	5.32	0–6.69	0.00	0–1.39	0.017
S100	250 μm radius	n/mm <sup>2</sup>	11541.07	0–58520.52	0.00	0–1370.85	0.031
		μm <sup>2</sup> /mm <sup>2</sup>	3.95	1.01–4.63	0.62	0–1.38	0.015
S100	500 μm radius	n/mm <sup>2</sup>	4.59	3.37–6.41	1.40	0.17–5.36	0.032
		μm <sup>2</sup> /mm <sup>2</sup>	19957.54	2767.2–66454.5	1991.17	144.91–5436.96	0.023

AF, atrial fibrillation; CHAT, choline acetyltransferase; GAP43, growth-associated protein 43; IQR, interquartile range; SD, standard deviation; TH, tyrosine hydroxylase.

**Heart rhythm.** The density of TH-positive nerves was increased in subjects with a history of AF. Additionally, the density of GAP43-positive nerves and S100-positive nerves was higher in subjects with AF compared to those without AF (Table 2A, Table S2, Figs 3 and 4, and Fig. S1). Taken together, subjects with AF had increased sympathetic innervation and neural growth in the VOM area.

**Myocardial infarction.** In subjects with histologically confirmed myocardial infarction, the density of TH-positive nerves, GAP43-positive nerves, and S100-positive nerves was increased in the VOM area (Table 2B, Table S3, Fig. 5, and Fig. S2). In summary, these results suggest increased sympathetic innervation and neural growth around the VOM in subjects with histologically verified myocardial infarction.

**Underlying cause of death.** Subjects with underlying cardiovascular cause of death had increased TH-positive nerve density. Similarly, CHAT-positive nerve density and S100-positive nerve density were increased in subjects with documented underlying cardiovascular cause of death compared to those with non-cardiovascular cause of death (Table 2C, Table S4, Figs 3 and 6, and Fig. S3). These results indicate increased overall autonomic innervation (both sympathetic and parasympathetic) around the VOM in subjects with underlying cardiovascular cause of death.

**Immediate cause of death.** The TH-positive nerve density was increased in subjects with immediate cardiovascular cause of death. A similar trend was seen in the density of GAP43-positive nerves and S100-positive nerves in subjects with immediate cardiovascular vs non-cardiovascular cause of death (Table 2D, Table S5, Figs 3 and 6, and Fig. S3). Overall, these results show increased sympathetic nerve density and neural growth around the VOM in subjects with immediate cause of death.

#### Interstitial fibrosis

The extent of interstitial fibrosis in the whole study population varied between 26.99 and 31.88%, depending on the proximity to the VOM (Table S1B). The interstitial fibrosis showed significant positive correlation with the age of subjects in all five regions of interest (250  $\mu$ m radius:  $r = 0.503$ ,  $p = 0.014$ ; 500  $\mu$ m radius:  $r = 0.560$ ,  $p = 0.005$ ; 1000  $\mu$ m radius:  $r = 0.577$ ,  $p = 0.004$ ; 1500  $\mu$ m radius:  $r = 0.547$ ,  $p = 0.007$ ; myocardium:  $r = 0.508$ ,  $p = 0.013$ ). Although there was an increased tendency of interstitial fibrosis observed

in subjects with a history of AF, these differences did not reach statistical significance. There was no association observed between the interstitial fibrosis and other available clinical data (heart weight, sex, cause of death, coronary atherosclerosis, dilatation of heart compartments, and myocardial infarction) (data not shown).

## DISCUSSION

### Major findings

In the present study, we quantified the distribution of autonomic nerves around the VOM, situated at an average distance of  $21.52 \pm 7.3$  mm distal to the VOM ostium, which corresponds to the level of the mitral isthmus [8]. We found predominant sympathetic innervation in all the studied regions adjacent to the VOM. The immunohistochemical evaluation of autonomic nerve density also revealed an increased density of sympathetic nerves and neural growth in subjects with AF, a history of cardiovascular immediate and underlying cause of death, and myocardial infarction. Interstitial myocardial fibrosis exhibited an age-related increase among the studied subjects. Heart weight was increased in subjects with a history of AF and with documented immediate cardiovascular cause of death. Lastly, the mean length of the patent VOM from its ostium was  $32.83 \pm 5.18$  mm, which is consistent with a previous study ( $30.8 \pm 13.6$  mm) [15].

### Autonomic innervation changes in the vein of Marshall area

#### Autonomic innervation topography

The LOM has been shown to be densely innervated by sympathetic and parasympathetic nerves and ganglia [2]. The nerves are connected with the atrioventricular node [7] and are important for regulating electrophysiological functions of the heart [16]. According to previous research, the distal part of LOM, reaching the left superior pulmonary vein, contains a high density of sympathetic nerves. The proximal portion of LOM, around the coronary sinus juncture, is innervated mainly by parasympathetic ganglia [17]. These findings were confirmed by an electrophysiological study [18] that reported a threshold stimulation gradient between the proximal and distal parts of the LOM. Thus, these studies support regional differences and a shift of autonomic innervation along the LOM area. In our study, we observed that the VOM area at the level of the mitral isthmus contained rich sympathetic (TH-positive) innervation. The sympathetic nerve density was more abundant in the myocardium,

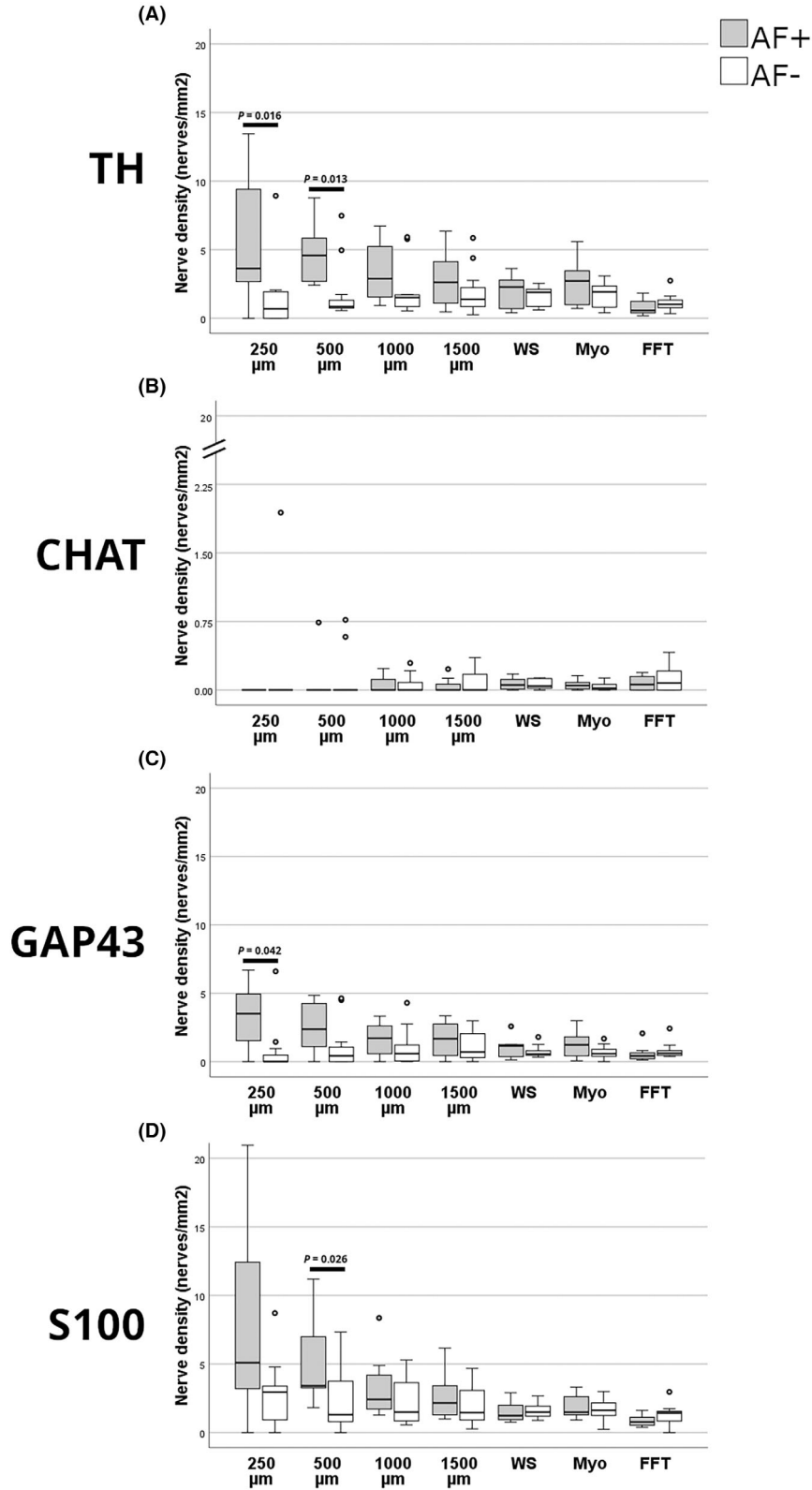




**Fig. 4.** Nerve densities around the VOM associated with heart rhythm: Box plot graphs representing interquartile range (box), 95% confidence interval (whiskers), and median (horizontal line inside the box) of nerve densities in seven studied regions of interest, divided by the presence of atrial fibrillation (AF<sup>+</sup>) or no history of atrial fibrillation (AF<sup>-</sup>). The nerve densities are expressed in nerves/mm<sup>2</sup>. Immunohistochemical stains: TH, tyrosine hydroxylase (A), CHAT, choline acetyltransferase (B), GAP43, growth-associated protein 43 (C), S100 (D). Statistically significant differences ( $p < 0.05$ ) are labeled by a bar and p-value. Studied regions: 250, 500, 1000, and 1500  $\mu\text{m}$  = expansion radiuses of 250–1500  $\mu\text{m}$  from the VOM; FFT, fibro-fatty tissue; Myo, myocardium; WS, whole slide.

fibro-fatty tissue, and all the regions within the expansion radiuses adjacent to the VOM, compared to the parasympathetic (CHAT-positive) nerves. These results may have implications for the topographical improvement of ethanol infusion or catheter ablation techniques targeting the autonomic nerves around the VOM and mitral isthmus, respectively, offering potential additional benefits for AF management. Moreover, ablation of the mitral isthmus is usually suitable for the prevention of atrial tachyarrhythmias respecting the preservation of atrial physiology [19] and considering our results may increase the effectiveness of the ablation strategy.

#### Autonomic innervation and atrial fibrillation

Previous research has established the implication of myocardial connections with the left atrium and autonomic stimulation in the LOM region [2] as possible mechanisms of AF. Activation of sympathetic nerves increases the influx and release of Ca<sup>2+</sup> from the sarcoplasmic reticulum and changes the refractory period of cardiomyocytes, leading to the initiation and perpetuation of AF [20]. Lin et al. [18] reported a gradient of AF inducibility with an increasing stimulation threshold from the proximal to the distal part of the LOM. Chang et al. [21] showed atrial sympathetic hyperinnervation and significant neural growth in a canine model of AF. These observations provide further support for the hypothesis that increased sympathetic innervation and neural growth around the VOM play an important role in the pathophysiology of AF and VOM ablation can effectively eliminate ectopic triggers by affecting the autonomic nervous system [3]. Consistent with the literature, this research found increased TH-, GAP43-, and S100-positive nerve density around the VOM in subjects with a history of AF. Interestingly, the number of sympathetic nerves was significantly increased within the expansion radiuses of 250 and 500  $\mu\text{m}$  to the VOM. According to these data, we can infer that altered sympathetic innervation and neural growth in direct proximity to the VOM at the level of the mitral isthmus are associated with AF. Showing histological differences around an anatomical area in patients with AF may explain, why surgical ablation often does not suffice to

prevent or cure AF. Therefore, the intervention should be extended to the VOM region.

#### Autonomic innervation and cardiovascular morbidity and mortality

In the current study, sympathetic innervation in the VOM area was increased in subjects with documented underlying cardiovascular cause of death. Additionally, subjects with histologically diagnosed myocardial infarction and immediate cardiovascular cause of death had significantly increased sympathetic innervation and neural growth in the atrial myocardium around the VOM. These findings might be explained by regeneration and active neural sprouting of sympathetic nerves after ischemic tissue damage [22] caused by various diseases affecting the myocardium. Increased sympathetic innervation was also observed in heart ventricles after ischemic injury and the nerve density was associated with ventricular tachyarrhythmias [23]. As shown in previous studies, myocardial infarction is associated with increased myocardial TH-, GAP43-, and S100-positive nerve density [23, 24]. Such dynamic innervation patterns vary in different cardiovascular diseases and may contribute to unpredictable neural activation with an increased risk of lethal arrhythmias [25]. Interestingly, a previous canine study reported abundant sympathetic nerve fibers in the distal part of the LOM, and ablation of the area reduced malignant arrhythmias experimentally induced by myocardial infarction and reperfusion [26]. The findings of the study suggest that the LOM ablation might be cardioprotective by impairing the sympathetic nerves innervating the ventricles. The clinical utility of cardiac autonomic innervation in the VOM area is therefore an important issue for future research on its potential role in the pathophysiology of cardiovascular morbidity and mortality, and suitable local therapeutic interventions.

#### Interstitial fibrosis

Cardiac interstitial fibrosis results from myocardial collagen accumulation and may lead to heart failure and increased cardiovascular morbidity and mortality [4]. Fibrotic remodeling of the myocardium is also associated with aging [6] as in the

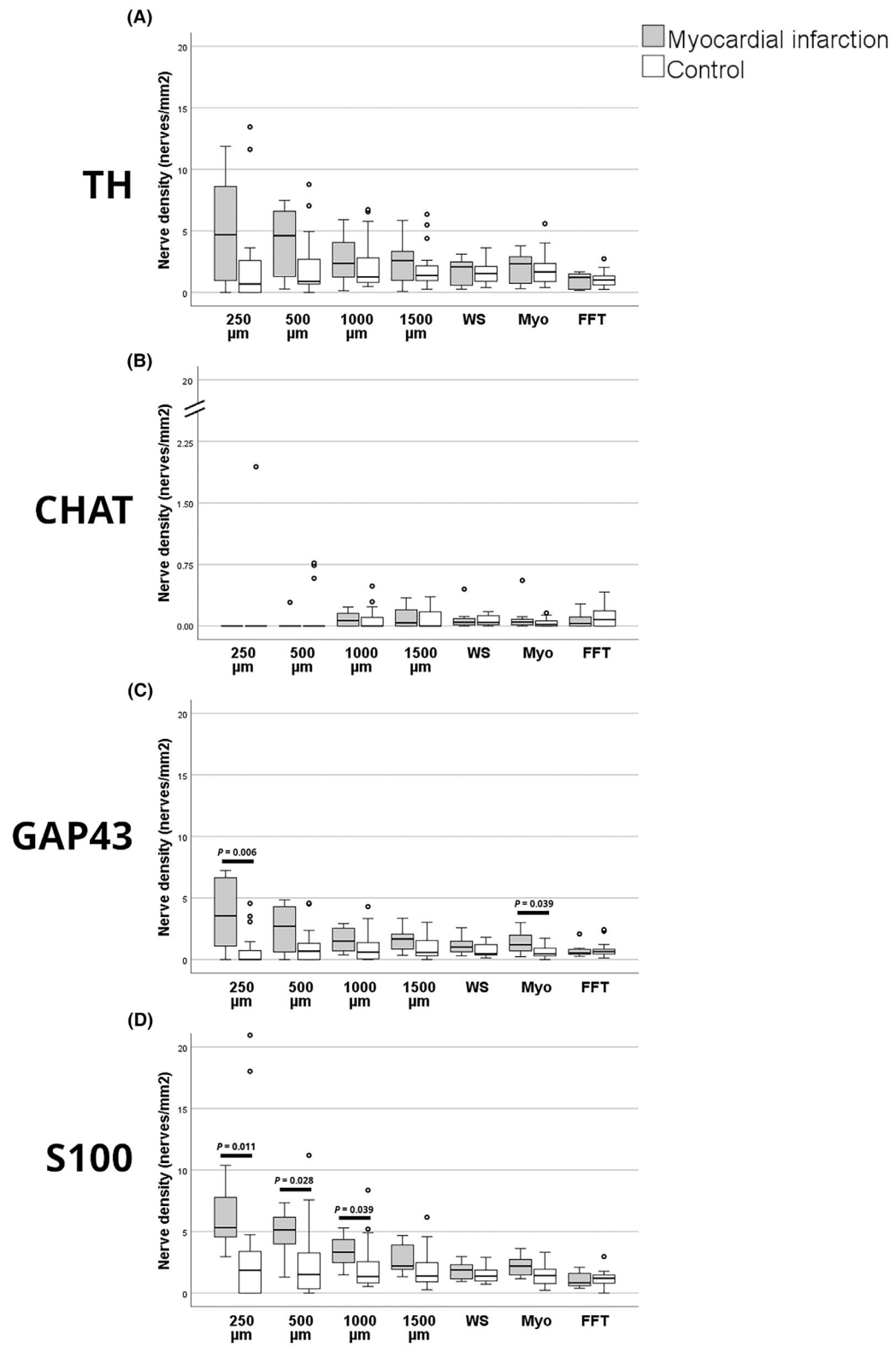


**Fig. 5.** Nerve densities around the VOM associated with myocardial infarction: Box plot graphs representing interquartile range (box), 95% confidence interval (whiskers), and median (horizontal line inside the box) of nerve densities in seven studied regions of interest, divided by subjects with microscopic myocardial infarction or those without. The nerve densities are expressed in nerves/mm<sup>2</sup>. Immunohistochemical stains: TH, tyrosine hydroxylase (A), CHAT, choline acetyltransferase (B), GAP43, growth-associated protein 43 (C), S100 (D). Statistically significant differences ( $p < 0.05$ ) are labeled by a bar and p-value. Studied regions: 250, 500, 1000, and 1500  $\mu\text{m}$  = expansion radiuses of 250–1500  $\mu\text{m}$  from the VOM; FFT, fibro-fatty tissue; Myo, myocardium; WS, whole slide.

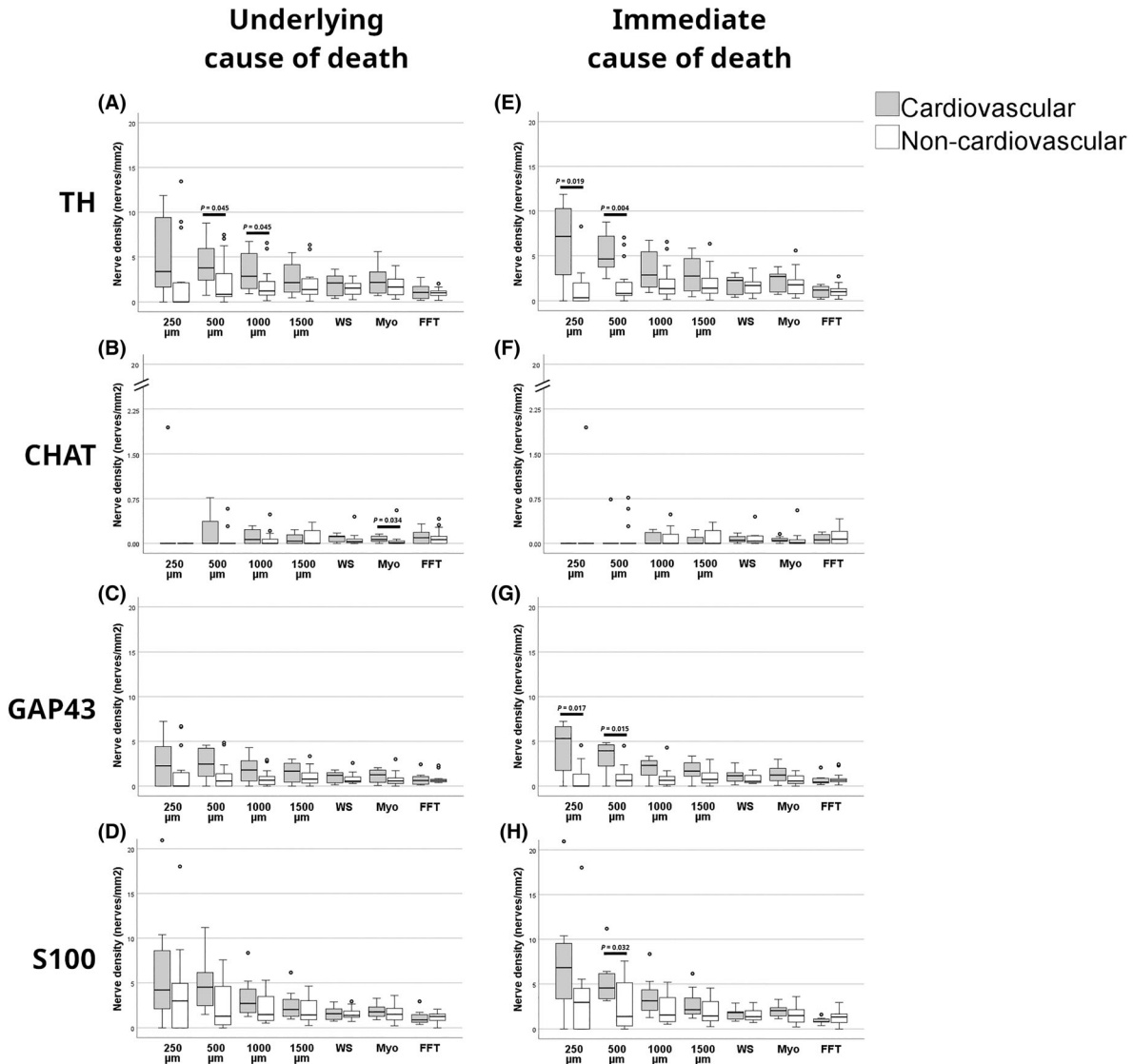


**Fig. 6.** Nerve densities around the VOM associated with underlying and immediate causes of death: Box plot graphs representing interquartile range (box), 95% confidence interval (whiskers), and median (horizontal line inside the box) of nerve densities in seven studied regions of interest, divided by cardiovascular or non-cardiovascular cause of death. The nerve densities are expressed in nerves/mm<sup>2</sup>. Immunohistochemical stains: TH, tyrosine hydroxylase (A, E), CHAT, choline acetyltransferase (B, F), GAP43, growth-associated protein 43 (C, G), S100 (D, H). Statistically significant differences ( $p < 0.05$ ) are labeled by a bar and p-value. Studied regions: 250, 500, 1000, and 1500  $\mu\text{m}$  = expansion radiuses of 250–1500  $\mu\text{m}$  from the VOM; FFT, fibro-fatty tissue; Myo, myocardium; WS, whole slide.

present study. In our series, increased fibrosis may be solely explained by the older age of the subjects, however, it also creates a possible link to the pathophysiology of atrial arrhythmias. Hassink *et al.* [5] reported increased fibrosis extent in the myocardium of pulmonary veins in human subjects with AF. A previous study quantitatively described the right atrial appendage transmural fibrosis profile of 17% and 27.5% in the control and AF groups, respectively, with decreasing content of fibrosis from the epicardium to the endocardium [27]. Moreover, Maesen *et al.* [28] suggested that endomyocardial, not overall myocardial fibrosis, plays a key role in the conduction disturbances in atrial fibrillation. These findings can be related to increased conduction resistance in fibrotic tissue slowing down the electric impulses. The current study demonstrates increased interstitial fibrosis around the VOM in subjects with AF, however, the difference was not statistically significant. Our results are in line with a previous study that reported myocardial structural changes in subjects with AF and found no association between myocardial fibrosis and AF [29].

#### Limitations of the study

We acknowledge the following potential limitations of the present study. Clinical data including heart rhythm history were collected from the autopsy referrals only and may be incomplete. Autonomic innervation of the heart can be influenced by many factors, including the pharmacologic therapy (e.g., beta-blockers) [30], aging and underlying health conditions [31]. Moreover, our results may have been constrained by the limited size of our study cohort, the relatively advanced age of the subjects, and variations in tissue sample sizes with an uneven innervation pattern. In addition, conclusions concerning atrial fibrillation may be limited due to the small number of AF subjects included in the study cohort as the material was prospectively collected from consecutive hospital autopsies and we could not influence the number of subjects with a history of AF. In our study cohort, 71.4% (5 out of 7) of subjects with a history of atrial fibrillation had documented cardiovascular causes of death, which may limit our conclusions concerning these two clinical entities. Further morphometric studies with more AF cases are thus needed to differentiate the role of AF and cardiovascular causes of death and prove their relationship with morphologic changes. The results of the current study do not provide detailed gross measurements of the VOM and coronary sinus in the studied subjects.

## CONCLUSIONS

Sympathetic innervation and neural growth changes around the VOM at the level of the mitral isthmus area were associated with AF, myocardial infarction, and cardiovascular cause of death. Aging was associated with increased interstitial fibrosis. Heart weight was increased in subjects with AF and cardiovascular causes of death. Although several questions remain to be answered, the study adds to a better understanding of the topography of cardiac autonomic innervation in the VOM area in various diseases and have implications for the development of new therapeutic approaches targeting the autonomic nervous system.

---

The authors appreciate the expert laboratory work of Sari Toivola and Eini Eskola (Tampere University, Tampere, Finland).

## CONFLICT OF INTEREST

The authors have no conflicts of interest to declare.

## AUTHOR CONTRIBUTIONS

All authors reviewed and approved the final version of the manuscript and meet the criteria for authorship. Specifically: Denis Depes designed the study, collected and analyzed the data, and wrote the manuscript. Ari Mennander contributed to data analysis and data interpretation. Paavo Immonen collected the data. Artturi Mäkinen acquired the tissue samples. Heini Huhtala provided valuable input for statistical analysis. Timo Paavonen designed and supervised the study. Ivana Kholová designed and supervised the study, and contributed to the interpretation of the data and drafting of the manuscript.

## FUNDING

This study was funded by grants from the Competitive Research Funding of the Pirkanmaa Hospital District (to IK, AM, TP), Tampere University Hospital Support Foundation (to IK), Aarne Koskelo Foundation (to IK, DD), Emil Aaltonen Foundation (to IK), Tampere Tuberculosis Foundation (to IK), Maire Taponen Foundation (to DD), Onni and Hilja Tuovinen Foundation (to DD), Päivikki and Sakari Sohlberg Foundation (to DD), and the



Research Foundation for Laboratory Medicine (to DD).

#### DATA AVAILABILITY STATEMENT

The data underlying this article are available in the article and in its online supplementary material.

#### REFERENCES

- Corradi D, Callegari S, Gelsomino S, Lorusso R, Macchi E. Morphology and pathophysiology of target anatomical sites for ablation procedures in patients with atrial fibrillation: part II: pulmonary veins, caval veins, ganglionated plexi, and ligament of Marshall. *Int J Cardiol.* 2013;168:1769–78.
- Makino M, Inoue S, Matsuyama TA, Ogawa G, Sakai T, Kobayashi YI, et al. Diverse myocardial extension and autonomic innervation on ligament of Marshall in humans. *J Cardiovasc Electrophysiol.* 2006;17:594–9.
- Valderrábano M, Peterson LE, Swarup V, Schurmann PA, Makkar A, Doshi RN, et al. Effect of catheter ablation with vein of Marshall ethanol infusion vs catheter ablation alone on persistent atrial fibrillation: the VENUS randomized clinical trial. *JAMA.* 2020;324:1620–8.
- Lu L, Guo J, Hua Y, Huang K, Magaye R, Cornell J, et al. Cardiac fibrosis in the ageing heart: contributors and mechanisms. *Clin Exp Pharmacol Physiol.* 2017;44:55–63.
- Hassink RJ, Aretz HT, Ruskin J, Keane D. Morphology of atrial myocardium in human pulmonary veins: a postmortem analysis in patients with and without atrial fibrillation. *J Am Coll Cardiol.* 2003;42:1108–14.
- Horn MA, Trafford AW. Aging and the cardiac collagen matrix: novel mediators of fibrotic remodelling. *J Mol Cell Cardiol.* 2016;93:175–85.
- Báez-Escudero JL, Keida T, Dave AS, Okishige K, Valderrábano M. Ethanol infusion in the vein of Marshall leads to parasympathetic denervation of the human left atrium: implications for atrial fibrillation. *J Am Coll Cardiol.* 2014;63:1892–901.
- Báez-Escudero JL, Morales PF, Dave AS, Sasaridis CM, Kim YH, Okishige K, et al. Ethanol infusion the vein of Marshall facilitates mitral isthmus ablation. *Heart Rhythm.* 2012;9:1207–15.
- Hindricks G, Potpara T, Dagres N, Arbelo E, Bax JJ, Blomström-Lundqvist C, et al. 2020 ESC guidelines for the diagnosis and management of atrial fibrillation developed in collaboration with the European Association for Cardio-Thoracic Surgery (EACTS). *Eur Heart J.* 2021;42:373–498.
- Michaud K, Basso C, d'Amati G, Giordano C, Kholová I, Preston SD, et al. Diagnosis of myocardial infarction at autopsy: AECVP reappraisal in the light of the current clinical classification. *Virchows Arch.* 2020;476:179–94.
- Basso C, Aguilera B, Banner J, Cohle S, d'Amati G, de Gouveia RH, et al. Guidelines for autopsy investigation of sudden cardiac death: 2017 update from the Association for European Cardiovascular Pathology. *Virchows Arch.* 2017;471:691–705.
- Depes D, Mennander A, Paavonen T, Kholová I. Autonomic nerves in myocardial sleeves around caval veins: potential role in cardiovascular mortality? *Cardiovasc Pathol.* 2022;59:107426.
- Depes D, Mennander A, Vehniäinen R, Paavonen T, Kholová I. Human pulmonary vein myocardial sleeve autonomic neural density and cardiovascular mortality. *J Histochem Cytochem.* 2022;70:627–42.
- Bankhead P, Loughrey MB, Fernández JA, Dombrowski Y, McArt DG, Dunne PD, et al. QuPath: open source software for digital pathology image analysis. *Sci Rep.* 2017;7:1–7.
- Zabówka A, Jakiel M, Bolechała F, Jakiel R, Jasińska KA, Hołda MK. Topography of the oblique vein of the left atrium (vein of Marshall). *Kardiol Pol.* 2020;78:688–93.
- Lin J, Scherlag BJ, Niu G, Lu Z, Patterson E, Liu S, et al. Autonomic elements within the ligament of Marshall and inferior left ganglionated plexus mediate functions of the atrial neural network. *J Cardiovasc Electrophysiol.* 2009;20:318–24.
- Rodríguez-Mañero M, Schurmann P, Valderrábano M. Ligament and vein of Marshall: a therapeutic opportunity in atrial fibrillation. *Heart Rhythm.* 2016;13:593–601.
- Lin J, Scherlag BJ, Lu Z, Zhang Y, Liu S, Patterson E, et al. Inducibility of atrial and ventricular arrhythmias along the ligament of Marshall: role of autonomic factors. *J Cardiovasc Electrophysiol.* 2008;19:955–62.
- Lai Y, Guo Q, Sang C, Gao M, Huang L, Zuo S, et al. Revisiting the characteristics and ablation strategy of biatrial tachycardias: a case series and systematic review. *Europace.* 2022;25:905–13.
- Patterson E, Lazzara R, Szabo B, Liu H, Tang D, Li YH, et al. Sodium-calcium exchange initiated by the Ca<sup>2+</sup> transient: an arrhythmia trigger within pulmonary veins. *J Am Coll Cardiol.* 2006;47:1196–206.
- Chang CM, Wu TJ, Zhou S, Doshi RN, Lee MH, Ohara T, et al. Nerve sprouting and sympathetic hyperinnervation in a canine model of atrial fibrillation produced by prolonged right atrial pacing. *Circulation.* 2001;103:22–5.
- Fu SY, Gordon T. The cellular and molecular basis of peripheral nerve regeneration. *Mol Neurobiol.* 1997;14:67–116.
- Cao JM, Fishbein MC, Han JB, Lai WW, Lai AC, Wu TJ, et al. Relationship between regional cardiac hyperinnervation and ventricular arrhythmia. *Circulation.* 2000;101:1960–9.
- Zhou S, Chen LS, Miyauchi Y, Miyauchi M, Kar S, Kangavari S, et al. Mechanisms of cardiac nerve sprouting after myocardial infarction in dogs. *Circ Res.* 2004;95:76–83.
- Fukuda K, Kanazawa H, Aizawa Y, Ardell JL, Shivkumar K. Cardiac innervation and sudden cardiac death. *Circ Res.* 2015;116:2005–19.
- Liu S, Yu X, Luo D, Qin Z, Wang X, He W, et al. Ablation of the ligament of Marshall and left stellate ganglion similarly reduces ventricular arrhythmias during acute myocardial infarction. *Circ Arrhythm Electrophysiol.* 2018;11:e005945.

27. Ravelli F, Masè M, Cristoforetti A, Avogaro L, D'Amato E, Tessarolo F, et al. Quantitative assessment of transmural fibrosis profile in the human atrium: evidence for a three-dimensional arrhythmic substrate by slice-to-slice histology. *Europace*. 2022;25:739–47.
28. Maesen B, Verheule S, Zeemering S, La Meir M, Nijss J, Lumeij S, et al. Endomysial fibrosis, rather than overall connective tissue content, is the main determinant of conduction disturbances in human atrial fibrillation. *Europace*. 2022;24:1015–24.
29. De Oliveira IM, Oliveira BD, Scanavacca MI, Gutierrez PS. Fibrosis, myocardial crossings, disconnections, abrupt turns, and epicardial reflections: do they play an actual role in human permanent atrial fibrillation? A controlled necropsy study. *Cardiovasc Pathol*. 2013;22:65–9.
30. Clarke GL, Bhattacharjee A, Tague SE, Hasan W, Smith PG.  $\beta$ -Adrenoceptor blockers increase cardiac sympathetic innervation by inhibiting autoreceptor suppression of axon growth. *J Neurosci*. 2010;30:12446–54.
31. Elia A, Cannavo A, Gambino G, Cimini M, Ferrara N, Kishore R, et al. Aging is associated with cardiac autonomic nerve fiber depletion and reduced cardiac and circulating BDNF levels. *J Geriatr Cardiol*. 2021;18:549–59.

## SUPPORTING INFORMATION

Additional supporting information may be found online in the Supporting Information section at the end of the article.

**Fig. S1.** Nerve densities around the VOM associated with heart rhythm: Box plot graphs representing interquartile range (box), 95% confidence interval (whiskers), and median (horizontal line inside the box) of nerve densities in seven studied regions of interest, divided by the presence of atrial fibrillation (AF+) or no history of atrial fibrillation (AF-). The nerve densities are expressed in  $\mu\text{m}^2/\text{mm}^2$ . Immunohistochemical stains: TH – tyrosine hydroxylase (A), CHAT – choline acetyltransferase (B), GAP43 – growth-associated protein 43 (C), and S100 (D). Statistically significant differences ( $P < 0.05$ ) are labeled by a bar and  $p$ -value. Studied regions: 250, 500, 1000, and 1500  $\mu\text{m}$  = expansion radiuses of 250–1500  $\mu\text{m}$  from the VOM; WS = whole slide; Myo = myocardium; FFT = fibro-fatty tissue.

**Fig. S2.** Nerve densities around the VOM associated with myocardial infarction: Box plot graphs representing interquartile range (box), 95%

confidence interval (whiskers), and median (horizontal line inside the box) of nerve densities in seven studied regions of interest, divided by subjects with microscopic myocardial infarction or those without. The nerve densities are expressed in  $\mu\text{m}^2/\text{mm}^2$ . Immunohistochemical stains: TH – tyrosine hydroxylase (A), CHAT – choline acetyltransferase (B), GAP43 – growth-associated protein 43 (C), and S100 (D). Statistically significant differences ( $p < 0.05$ ) are labeled by a bar and  $p$ -value. Studied regions: 250, 500, 1000, and 1500  $\mu\text{m}$  = expansion radiuses of 250–1500  $\mu\text{m}$  from the VOM; WS = whole slide; Myo = myocardium; FFT = fibro-fatty tissue.

**Fig. S3.** Nerve densities around the VOM associated with underlying and immediate causes of death: Box plot graphs representing interquartile range (box), 95% confidence interval (whiskers), and median (horizontal line inside the box) of nerve densities in seven studied regions of interest, divided by cardiovascular or non-cardiovascular cause of death. The nerve densities are expressed in  $\mu\text{m}^2/\text{mm}^2$ . Immunohistochemical stains: TH – tyrosine hydroxylase (A, E), CHAT – choline acetyltransferase (B, F), GAP43 – growth-associated protein 43 (C, G), and S100 (D, H). Statistically significant differences ( $P < 0.05$ ) are labeled by a bar and  $p$ -value. Studied regions: 250, 500, 1000, and 1500  $\mu\text{m}$  = expansion radiuses of 250–1500  $\mu\text{m}$  from the VOM; WS = whole slide; Myo = myocardium; FFT = fibro-fatty tissue.

**Table S1.** Morphometric analysis of the vein of Marshall (VOM). Data show overall nerve density and interstitial fibrosis in studied regions around the VOM. A: nerve densities, B: interstitial fibrosis.

**Table S2.** Comparison table of nerve densities between subjects with atrial fibrillation and without atrial fibrillation.

**Table S3.** Comparison table of nerve densities between subjects with histologically verified myocardial infarction and controls.

**Table S4.** Comparison table of nerve densities between subjects with documented underlying cardiovascular and non-cardiovascular cause of death.

**Table S5.** Comparison table of nerve densities between subjects with documented immediate cardiovascular and non-cardiovascular cause of death.